

Exact Estimation of Multiple Directed Acyclic Graphs

Chris. J. Oates*, Jim Q. Smith*, Sach Mukherjee†, James Cussens‡

April 20, 2017

Abstract

Probability models based on directed acyclic graphs (DAGs) are widely used to make inferences and predictions concerning interplay in multivariate systems. In many applications, data are collected from related but non-identical units whose DAGs may differ but are likely to share many features. Statistical estimation for multiple related DAGs appears extremely challenging since all graphs must be simultaneously acyclic. Recent work by Oyen and Lane (2013) avoids this problem by making the strong assumption that all units share a common ordering of the variables and that this ordering is known to the statistician. In this paper we propose a novel Bayesian formulation for multiple DAGs and, requiring no assumptions on any ordering of the variables, we prove that the *maximum a posteriori* estimate is characterised as the solution to an integer linear program (ILP). Consequently estimation may be achieved using highly optimised techniques for ILP instances, including constraint propagation and cutting plane algorithms. Our framework permits a complex dependency structure on the collection of units, including group and subgroup structure. This dependency structure can itself be efficiently learned from data and a special case of our methodology provides a novel analogue of k -means clustering for DAGs. Results on simulated data and fMRI data obtained from multiple subjects are presented.

1 Introduction

Probabilistic graphical models are widely used to model interplay in multivariate systems. In brief, vertices in a graph G are identified with random variables and edges between the vertices describe conditional independence statements, whose interpretation depends on both the statistical model and the scientific context. In many applications the graph structure itself is uncertain and an important challenge is to infer this structure from experimental data. There has been considerable research into inference for graphical models over the last decade, with particular emphasis on Bayesian networks (BNs; Friedman and Koller, 2003; Ellis and Wong, 2008; He *et al.*, 2013), Gaussian graphical models (GGMs; Meinshausen and Bühlmann, 2006; Chandrasekaran *et al.*, 2012) and discrete graphical models (Loh and Wainwright, 2013). Nevertheless there remain two substantive barriers to the inference of graphical models from data:

1. **Robustness.** It is often the case that inferred graphical structure is not robust to reasonable perturbation of the underlying data (Claassen and Heskes, 2012). This is due to a combination of (1) the high variance of graphical estimators themselves and (2) additional variance that is introduced if the structure learning algorithm returns only an approximation to the intended estimator.
2. **Small sample bias.** Conventional model selection criteria for graphical models are often biased towards selecting more complex models (i.e. more edges), since there are typically very many models in which the data-generating model is nested; these models are also able to fit the data well (albeit with some coefficients close or equal to zero Consonni and La Rocca, 2010). Consequently many more data are required to exclude more complex alternatives.

*Dept. Statistics, University of Warwick

†MRC Biostatistics Unit and CRUK Cambridge Institute

‡Dept. Computer Science and Centre for Complex Systems Analysis, University of York

In many applications, data are collected on multiple units $k \in \{1, 2, \dots, K\}$ that may differ with respect to interplay between variables, such that corresponding networks $G^{(k)}$ may be unit-specific. For example, in biology, units may correspond to different patients, cell lines or replicate experiments and the graphs themselves may describe gene regulation or protein signalling pathways. Interplay in cellular systems can depend on the genetic and epigenetic state of the units, such that even for a well-defined system, such as signalling in response to ligand stimulation, or regulation of a gene by transcription factors, details may differ between even closely related samples (Ideker and Krogan, 2012; Csermely, 2013). Furthermore, the availability of increasingly high-throughput biochemical assays has led to an increase in experimental designs that include panels of potentially heterogeneous units (Cao *et al.*, 2011; Barretina *et al.*, 2012; Maher, 2012; The Cancer Genome Atlas Network, 2012). In such settings there is scientific interest in unit-specific networks $G^{(k)}$ as well as their similarities and differences.

In the context of inference for multiple related graphical models, it is natural to leverage the similarity between units in order to both (1) improve robustness of inferred graphical structure and (2) to reduce small sample bias through information sharing. This approach has recently received much attention: For GGMs, Chiquet *et al.* (2011); Hara and Washio (2012); Mohan *et al.* (2012); Yang *et al.* (2012); Danaher *et al.* (2014) exploit L_1 penalties to couple together inference for multiple related units. This methodology addresses the first component of robustness discussed above by requiring that graphical structure is approximately invariant to perturbations of the data that are, in effect, provided by the multiple related units. Such algorithms are exact, addressing the second component of robustness discussed above, and scale well to high dimensions. Supporting empirical evidence suggests that it is possible to reduce small sample bias, often considerably, by formulating an appropriate joint model that couples together multiple units. For emerging datasets the number of units K is often very large; in biology for example $K = 947$ (Barretina *et al.*, 2012), $K = 80$ (Cao *et al.*, 2011), $K = 150$ (Maher, 2012), $K \approx 500$ (The Cancer Genome Atlas Network, 2012), so that joint estimation could be expected to provide significant gains.

This paper focusses instead on models that are characterised by DAGs. Specifically, consider a fixed unit and let $Y_i(n)$ be a random variable representing the n th observation of variable i for this unit. The methodology that we present applies to DAG models for which the conditional distribution of the variables \mathbf{Y} , given a DAG G and associated parameters $\boldsymbol{\theta}$, factorises as

$$p(\mathbf{Y}|\boldsymbol{\theta}, G) = \prod_{i=1}^P \prod_{n=1}^N p(Y_i(n)|\mathbf{Y}_{G_i}(n), \boldsymbol{\theta}_i(n), G_i). \quad (1)$$

Here G_i are the parents of variable i according to G and $\mathbf{Y}_{G_i}(n)$ are the observed values of these parents in sample n . Additionally, $\boldsymbol{\theta}_i$ are parameters associated with the conditional distribution for variable i that may depend on sample index n model G_i though this is suppressed in the notation. The best known class of models that satisfy Eqn. 1 are BNs. BNs are a popular class of graphical models that, unlike GGMs, admit an extensive theory of inferred causation (Pearl, 2009). In particular BNs allow estimation of interventional distributions and causal effects that are the objects of interest in numerous scientific applications (e.g. Sachs *et al.*, 2005; Maathuis *et al.*, 2009; Peters *et al.*, 2011). The ability to jointly estimate multiple BNs in an exact manner is highly desirable, due to both a sophisticated theoretical understanding of individual BNs and the rapid emergence of large heterogeneous experimental data. An exact algorithm has not yet been discovered and even approximate joint inference for multiple BNs is currently extremely computationally challenging. This contrasts with inference for individual BNs where extremely efficient algorithms based on ILP have been developed (Bartlett and Cussens, 2013). An algorithm for exact estimation of multiple BNs, or more general DAG models, is the contribution of this research.

In addition to algorithmic development, we introduce a more general statistical framework for multiple graphical models than has previously been considered. Existing literature has restricted attention to the special case where the graphs $G^{(k)}$ are exchangeable, in the sense that all pairs of units undergo an equal amount of regularisation (Werhli and Husmeier, 2008; Chiquet *et al.*, 2011; Yang *et al.*, 2012; Mohan *et al.*, 2012; Penfold *et al.*, 2012; Oates *et al.*, 2013; Danaher *et al.*, 2014). However, in practice, relationships between datasets $\mathbf{Y}^{(k)}$ (and their underlying graphical models) may be complex, e.g. hierarchical, with group and sub-group structure. For example, in biology, datasets from multiple species may be related according

to a complex evolutionary history (Baumbach *et al.*, 2009), while cancer cells are related according to their disease taxonomies (Curtis *et al.*, 2012). A common property of these examples is that in each case the relationships between units are themselves subject to uncertainty; it is therefore desirable to be able to simultaneously estimate unit-specific graphical models $G^{(k)}$ and the interdependency structure that relates the units themselves. Mukherjee and Hill (2011) formulated an approach to model-based clustering that focussed on GGMs, whilst Oates and Mukherjee (2014) performed exact inference for nonexchangeable dynamic BNs under the strong assumption that the relationships between units are known. However we are unaware of any attempt to address nonexchangeability in the context of general DAG models. In this contribution we describe a formal statistical model for nonexchangeable DAGs and focus on the *maximum a posteriori* (MAP) estimator that simultaneously learns both unit-specific DAGs and the possibly complex interdependency structure that relates them.

The joint estimation of multiple DAGs, exact or otherwise, has so far received little attention. The first discussion of this problem that we are aware of occurred in Niculescu-Mizil and Caruana (2007); here a greedy search was used to locate a local maximum of a joint Bayesian posterior under the assumption that the pairs $(\mathbf{Y}^{(k)}, G^{(k)})$ may be treated as exchangeable random variables. Werhli and Husmeier (2008) described a Markov chain Monte Carlo (MCMC) technique for Bayesian inference that targets a joint posterior over (exchangeable) graphical structures; this is computationally very demanding since MCMC proposals in discrete state spaces often entail a low acceptance probability and the joint space of DAGs contains $\mathcal{O}((P!2^P)^K)$ elements where P is the number of nodes in each graph. Oyen and Lane (2013) recently proposed an exact method based on Bayesian model averaging, under the strong assumption that an ordering of the variables $1, \dots, P$ is known *a priori*, and that the same ordering applies simultaneously to all units (who are again modelled as exchangeable). For the specific class of “feed-forward” dynamic BNs, Oates *et al.* (2013) provides an exact belief propagation algorithm in the joint setting; however this approach does not generalise to arbitrary BNs since it implicitly requires a known ordering of the variables that is provided by the time index. The present contribution considerably extends these earlier research efforts by facilitating exact, computationally efficient inference over the full joint space of all possible combinations of DAGs. Moreover we require no assumptions on exchangeability on the units, nor that there is a fixed, known ordering of the variables.

Complementary research focusses on embellishing classical BNs with additional information to encode “context-specific” graphical structure (Boutilier *et al.*, 1996; Geiger and Heckerman, 1996; Pensar *et al.*, 2013). Thiesson *et al.* (1998) introduced BN mixture models; here each unit k is assigned a class label $Z^{(k)} \in \{1, \dots, L\}$ that denotes group membership; units in the same mixture component are modelled by the same graphical structure ($Z^{(k)} = Z^{(l)} \implies G^{(k)} = G^{(l)}$). The objects of inference are now the pairs $(G^{(k)}, Z^{(k)})$ and usually also the number L of mixture components. We demonstrate below that mixtures of BNs form a special case of our proposed methodology, thereby extending the use of ILP techniques also to this model class. Our work differs from embellishment techniques by focussing on regularisation between units based *only* on graphical structure; i.e. we do not require exchangeability assumptions on the mechanisms that underly conditional distributions within units, for example.

The remainder of the paper is organised as follows: In section 2 we introduce a novel statistical model for multiple (possibly nonexchangeable) DAGs that satisfy the factorisation of Eqn. 1 and discuss methods for regularisation based on graphical structure. Section 3 contains the core of our novel contribution, proving that MAP estimators can be exactly characterised as ILPs. Section 4 presents a simulation study and results on fMRI data obtained in a multi-subject study, where joint estimation can be expected to yield statistical gains. Finally we close with a discussion of directions for further research.

2 A Statistical Model for Multiple DAGs

We begin by introducing our estimators from a probabilistic perspective, deferring a discussion of statistical estimation until the next section. Throughout the shorthand $1 : P$ will be used to denote the list of integers $1, 2, \dots, P$. A (directed) graph G on vertices $1 : P$ is characterised by a collection of sets G_i , such that $G_i \subseteq \{1 : P\} \setminus \{i\}$ contains precisely the parents of vertex i according to G . We say G is acyclic if G

contains no sequence of directed edges that begins and ends at the same vertex and write \mathcal{G} for the space of all directed acyclic graphs (DAGs). In this paper the vertices i in a DAG G will be associated with random variables Y_i . We will use the shorthand $\mathbf{Y}_\pi^{(k)}(n)$ to represent the n th observation of all variables $\pi \subseteq \{1 : P\}$ taken from unit k .

Our methodology is presented from a Bayesian perspective, but can be equally motivated as a penalised likelihood approach. Below we introduce a prior distribution over all DAGs $G^{(1:K)} \in \mathcal{G}^K$ that encodes the notion of dependency that we wish to exploit during estimation. Write \mathcal{A} for the space of undirected networks on vertices $1 : K$. The “multiple DAG prior” that we propose factorises along edges of a network $A \in \mathcal{A}$ whose K vertices correspond to the individual units:

$$p(G^{(1:K)}|A) \propto \left(\prod_{(k,l) \in A} r(G^{(k)}, G^{(l)}) \right) \times \left(\prod_{k=1}^K m(G^{(k)}) \right) \quad (2)$$

Here the first product ranges over all edges (k, l) in the network A . The function $r(G^{(k)}, G^{(l)})$ is interpreted as a measure of “regularity” between the DAGs $G^{(k)}$ and $G^{(l)}$; specific choices for this function are discussed in section 2.1 below. The network A is therefore a representation of pairs of units that are *a priori* considered to have similar graphical structure (Fig. 1). For example, A may describe a time-ordering of the datasets, such that consecutive datasets are expected to have more similar graphical structures, or may indicate group membership within a mixture model. In all existing literature on the joint estimation of multiple graphical models, including BNs and GGMs, as far as we are aware, an exchangeability assumption is placed on $G^{(1:K)}$ that corresponds (implicitly) to specifying A as the complete network (Werhli and Husmeier, 2008; Chiquet *et al.*, 2011; Yang *et al.*, 2012; Mohan *et al.*, 2012; Penfold *et al.*, 2012; Oates *et al.*, 2013; Danaher *et al.*, 2014). By accommodating general $A \in \mathcal{A}$ we significantly extend the scientific applicability of graphical techniques to include potentially heterogeneous populations with a complex dependency structure. The remaining terms $m(G^{(k)})$ are necessary for multiplicity correction, which will be discussed in section 2.2 below.

The likelihood we consider follows from Eqn. 1 and the assumption that the observations $\mathbf{Y}^{(k)}$ are conditionally independent given the DAGs $G^{(k)}$ and associated parameters $\boldsymbol{\theta}^{(k)}$. Specifically, we have that the full likelihood factorises over units, variables and samples:

$$p(\mathbf{Y}^{(1:K)}|\boldsymbol{\theta}^{(1:K)}, G^{(1:K)}) = \prod_{k=1}^K \prod_{i=1}^P \prod_{n=1}^N p(Y_i^{(k)}(n)|\mathbf{Y}_{G_i^{(k)}}^{(k)}(n), \boldsymbol{\theta}_i^{(k)}(n), G_i^{(k)}) \quad (3)$$

For simplicity of presentation, we will assume that the same experimental design was used for each unit, so that in particular the number N of samples is the same for each unit, though this is not required for our methodology.

Within a Bayesian framework we place a prior distribution $p(\boldsymbol{\theta}_i^{(k)}|G_i^{(k)})$ over parameters $\boldsymbol{\theta}_i^{(k)}$, such that parameter sets corresponding to units k and l are independent conditional upon the two DAGs $G^{(k)}$ and $G^{(l)}$. Integrating out the unknown parameters provides the “evidence” in favour of the joint model $G^{(1:K)} \in \mathcal{G}^K$:

$$p(\mathbf{Y}^{(1:K)}|G^{(1:K)}, A) = \int p(\mathbf{Y}^{(1:K)}|\boldsymbol{\theta}^{(1:K)}, G^{(1:K)})p(\boldsymbol{\theta}^{(1:K)}|G^{(1:K)})d\boldsymbol{\theta}^{(1:K)} \quad (4)$$

In this paper we consider the challenge of estimating the MAP estimator for which observations $\mathbf{Y}^{(1:K)}$ provide the most evidence, subject to the multiple DAG prior:

$$\hat{G}^{(1:K)}|A := \arg \max_{G^{(1:K)} \in \mathcal{G}^K} p(G^{(1:K)}|\mathbf{Y}^{(1:K)}, A) \quad (5)$$

When A is the complete network we refer to inference as “exchangeable learning”. More generally, we consider the setting where A itself must be estimated from data. When A is uncertain we impose a prior

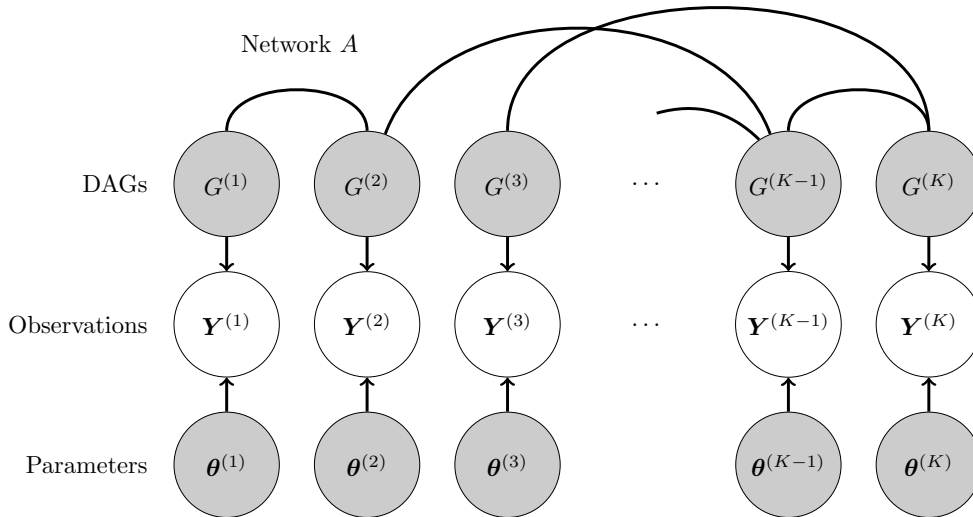


Figure 1: A hierarchical model for multiple directed acyclic graphics (DAGs), with relationships between DAGs encoded by an undirected network A . [Shaded nodes are unobserved. $G^{(1:K)}$ = data-generating graphs, $\theta^{(1:K)}$ = data-generating parameters, $\mathbf{Y}^{(1:K)}$ = observation vectors.]

distribution over $A \in \mathcal{A}$ (described in section 2.3) and refer to inference as “nonexchangeable learning”. In this extended setting, our focus is the MAP estimator

$$(\hat{G}^{(1:K)}, \hat{A}) := \arg \max_{\substack{G^{(1:K)} \in \mathcal{G}^K \\ A \in \mathcal{A}}} p(G^{(1:K)}, A | \mathbf{Y}^{(1:K)}). \quad (6)$$

One of the main contributions of this paper, in section 3, is to prove that for certain choices of the regularity function $r(G^{(k)}, G^{(l)})$ discussed below, both $\hat{G}^{(1:K)} | A$ and $(\hat{G}^{(1:K)}, \hat{A})$ are exactly characterised as the solutions to ILPs and hence are amenable to exact computation using advanced techniques such as constraint propagation and cutting plane algorithms.

2.1 A Default Choice of Regularity Function

Below we discuss choices for the regularity function $r(G^{(k)}, G^{(l)})$ that forms the basis for the multiple DAG prior and measures the amount of similarity between DAGs $G^{(k)}$ and $G^{(l)}$. Hyper-Markov laws form natural priors for a conjugate Bayesian analysis and are frequently employed in the context of graphical models to reduce the computational burden (Dawid and Lauritzen, 1993). The default choice that we consider for the regularity function is given by

$$\log(r(G^{(k)}, G^{(l)})) = - \sum_{i=1}^P \sum_{j=1}^P \lambda_{j,i}^{(k,l)} [(j \in G_i^{(k)}) \oplus (j \in G_i^{(l)})]. \quad (7)$$

Here \oplus is the logical XOR operator, $[E] \in \{0, 1\}$ is an indicator function associated with the event E and the $\lambda_{j,i}^{(k,l)}$ are (constant) penalty terms associated with the inclusion of the edge (j, i) in precisely one of the DAGs $G^{(k)}$ and $G^{(l)}$. Combined with the default multiplicity correction discussed below, the prior defined by Eqn. 7 is hyper-Markov with respect to *any* DAG $G^{(k)}$ when $G^{(l)}$ is held fixed; we will see in section 3 that such priors permit a particularly simple construction of an ILP for the multiple DAG model. For many scientific applications where graph structure represents a physical mechanism, Eqn. 7 arises naturally from simple physical considerations. For example in neuroscience, an edge in a graphical model corresponds to

physical connectivity and the transfer of information between regions of the brain (Costa *et al.*, 2013), or in molecular biology, an edge in a graphical model of protein signalling is interpreted as the occurrence of chemical reactions that involve both the parent and the child (Bowsher, 2010).

A specific instance of this approach, that treats both units and edges as exchangeable, is “structural Hamming distance” (SHD) given by $\lambda_{j,i}^{(k,l)} = \lambda \in [0, \infty) \forall i, j, k, l$. SHD has previously been used to regularise between graphical models by Niculescu-Mizil and Caruana (2007); Penfold *et al.* (2012); Oyen and Lane (2013); Oates *et al.* (2013) and to integrate prior knowledge into BNs by Acid and de Campos (2003); Tsamardinos *et al.* (2006); Perrier *et al.* (2008); Mukherjee and Hill (2011). An extension of SHD with two degrees of freedom was considered by Werhli and Husmeier (2008). This paper focusses on SHD due to its interpretability and simplicity, but the proposed methodology is compatible with Eqn. 7 and the constants $\lambda_{j,i}^{(k,l)}$ could be used to encode prior information on the similarity between units or the propensity for a particular edge to be shared between units.

2.2 A Default Choice of Multiplicity Correction

The function $m(G)$ in the multiple DAG prior (Eqn. 2) is required to adjust for the fact that the size of the space \mathcal{G} grows super-exponentially with the number P of vertices (Scott and Berger, 2010; Consonni and La Rocca, 2010; Oates and Mukherjee, 2014). In this paper we follow Scott and Berger (2010) and control multiplicity using the default correction

$$m(G) = \prod_{i=1}^P m_i(G_i), \quad m_i(\pi) = \binom{P}{|\pi|}^{-1} \mathbb{1}[|\pi| \leq d_{\max}]. \quad (8)$$

Here d_{\max} is a fixed upper bound on the in-degree of vertices in G that encodes prior knowledge on the support of \mathcal{G} , and is widely used to mediate computational intensity in practice (e.g. Hill *et al.*, 2012). This specification has the desirable property that the collective prior probability of all models with d predictors is $(1 + d_{\max})^{-1}$, which is independent of both d and P .

We note that the methodology presented in this paper is compatible with the inclusion of additional terms in Eqn. 2 that encode subjective prior structural information on the unit-specific DAGs (Mukherjee and Speed, 2008). For simplicity of exposition we assume no specific structural knowledge in the examples below.

2.3 A Default Choice of Hyperprior

We proceed to formulate a Bayesian prior distribution over networks $A \in \mathcal{A}$ that encodes prior knowledge of the interdependency structure that relates units $1, \dots, K$. To specify a default prior, we note that removal of an edge from A leads to reduced regularisation and improved fit-to-data. Write $\stackrel{+C}{=}$ for equality up to an unspecified additive constant. We proceed by placing a prior distribution on A that deters sparsity:

$$\log(p(A)) \stackrel{+C}{=} \sum_{k=1}^K \sum_{l=k+1}^K \eta^{(k,l)} \mathbb{1}[(k, l) \in A]. \quad (9)$$

Here the $\eta^{(k,l)}$ are (constant) reward terms associated with the inclusion of the edge (k, l) in the network A and could encode prior information regarding the similarity between units. (By convention the adjacency matrix corresponding to the network A is upper triangular, i.e. $k < l$.) As before, for simplicity we restrict attention to the default choice $\eta^{(k,l)} = \eta \in [0, \infty) \forall k, l$, but this is not required by our methodology. Here η is an inverse temperature hyperparameter that will help to determine the density of \hat{A} , with larger values of η representing *a priori* denser networks.

3 MAP Estimators for Multiple DAGs are ILPs

In this section we prove that MAP estimators for the multiple DAG model are exactly characterised as ILPs and hence admit advanced computational techniques for solving ILP instances.

Structure learning for individual DAGs is a well-studied problem, with contributions including Friedman and Koller (2003); Silander and Myllymäkki (2006); Tsamardinos *et al.* (2006); Cowell (2009); Cussens (2011); Yuan and Malone (2013). Our methodology is based upon the ILP approach to discrete optimisation for which there exist powerful techniques for efficient and exact solving (Nemhauser and Wolsey, 1988; Wolsey, 1998; Achterberg, 2009). In brief, an ILP takes the form

$$\text{maximise } \mathbf{f}^T \mathbf{x} \text{ subject to } \mathbf{A}\mathbf{x} \leq \mathbf{b}, \mathbf{C}\mathbf{x} = \mathbf{d}, \mathbf{x} \geq \mathbf{0}. \quad (10)$$

Here \mathbf{A} , \mathbf{C} are matrices and \mathbf{b} , \mathbf{d} are column vectors that together define linear (in-) equalities that an e -dimensional state vector $\mathbf{x} \in \mathbb{Z}^e$ must satisfy. Cussens (2010) and Jaakola *et al.* (2010) originally and independently demonstrated that the MAP estimator for an individual BN can be characterised as an ILP of the form Eqn. 10. Theoretical and computational advances (Bartlett and Cussens, 2013) have rendered ILPs a highly efficient and therefore attractive methodology for estimation in graphical models. The algorithms below extend the ILP approach to the more general setting of multiple DAG models.

3.1 Exact Estimation of Multiple DAGs When A is Known

In this section we consider the case where the network A is known *a priori*. We explicitly construct an ILP and prove that its solution is exactly the MAP estimator $\hat{G}^{(1:K)}|A$. Our methodology extends the ILP formulation of Jaakola *et al.* (2010) to multiple networks via the inclusion of additional state variables that capture the similarities and differences between graphical models.

We begin by computing and caching the terms

$$p(\mathbf{Y}_i^{(k)} | \mathbf{Y}_{G_i^{(k)}}^{(k)}, G_i^{(k)}) = \int p(\mathbf{Y}_i^{(k)} | \mathbf{Y}_{G_i^{(k)}}^{(k)}, \boldsymbol{\theta}_i^{(k)}, G_i^{(k)}) p(\boldsymbol{\theta}_i^{(k)} | G_i^{(k)}) d\boldsymbol{\theta}_i^{(k)} \quad (11)$$

that summarise evidence in the data for the local model $G_i^{(k)}$ for variable i in unit k . These are available in closed form for many models of interest, including but not limited to discrete BNs with Dirichlet priors (Heckerman *et al.*, 1995), linear Gaussian structural equation models (Pearl, 2009) and multiregression dynamical models (Queen and Smith, 1993). Since our approach is based upon these pre-computed quantities, they could even be obtained (for more complex models) numerically using MCMC and related techniques (e.g. Scheines *et al.*, 1999; Xu *et al.*, 2010). These cached quantities are transformed to obtain “local scores”

$$s^{(k)}(i, G_i^{(k)}) := \log(p(\mathbf{Y}_i^{(k)} | \mathbf{Y}_{G_i^{(k)}}^{(k)}, G_i^{(k)})) + \log(m_i(G_i^{(k)})). \quad (12)$$

These are the (log-) evidence from Eqn. 11 with an additional penalty term that provides multiplicity correction over varying $G_i^{(k)} \subseteq \{1 : P\} \setminus \{i\}$.

We define binary indicator variables that form the basis of our ILP as follows:

$$\Pi^{(k)}(i, \pi) := [G_i^{(k)} = \pi] \quad \forall i, k, \pi. \quad (13)$$

Here $\pi \subseteq \{1 : P\} \setminus \{i\}$ is used to denote a possible parent set for variable i in the DAG for unit k , so the information in the variables $\Pi^{(k)}$ completely characterises $G^{(k)}$. It will be necessary to impose constraints that ensure the $\Pi^{(k)}$ correspond to well-defined DAGs:

$$\sum_{\pi \subseteq \{1:P\} \setminus \{i\}} \Pi^{(k)}(i, \pi) = 1 \quad \forall i, k \quad (\text{C1; convexity})$$

Constraint (C1) requires that for each unit k , every vertex i has exactly one parent set (i.e. there is a well-defined graph $G^{(k)}$). To ensure $G^{(k)}$ is acyclic we require further constraints:

$$\sum_{i \in C} \sum_{\substack{\pi \subseteq \{1:P\} \setminus \{i\} \\ \pi \cap C = \emptyset}} \Pi^{(k)}(i, \pi) \geq 1 \quad \forall k, \emptyset \neq C \subseteq \{1:P\}. \quad (\text{C2; acyclicity})$$

(C2) states that for every non-empty set C there must be at least one vertex in C that does not have a parent in C . It was proven in Jaakola *et al.* (2010) that (C1-2) exactly characterise the space \mathcal{G} of DAGs.

An indicator of the presence of a specific edge (j, i) in $G^{(k)}$ is formed from the parent set indicators $\Pi^{(k)}$ as

$$e^{(k)}(j, i) := \sum_{\substack{\pi \subseteq \{1:P\} \setminus \{i\} \\ j \in \pi}} \Pi^{(k)}(i, \pi) \quad \forall i, j, k. \quad (\text{C3})$$

To decide whether units k, l agree on the presence or absence of a specific edge (j, i) , we introduce additional variables:

$$d^{(k,l)}(j, i) := [(j \in G_i^{(k)}) \oplus (j \in G_i^{(l)})] \quad \forall i, j, k, l \text{ with } k < l \quad (\text{C4})$$

Theorem 1. *The MAP estimate $\hat{G}^{(1:K)}|A$ is characterised as the solution of the ILP*

$$\hat{G}^{(1:K)}|A = \arg \max_{G^{(1:K)} \in \mathcal{G}^K} \sum_{k=1}^K \sum_{i=1}^P \sum_{\pi \subseteq \{1:P\} \setminus \{i\}} s^{(k)}(i, \pi) \Pi^{(k)}(i, \pi) - \lambda \sum_{(k,l) \in A} \sum_{i=1}^P \sum_{j=1}^P d^{(k,l)}(j, i) \quad (14)$$

subject to constraints (C1-4).

The proofs for this paper are provided in Appendix A. On the surface, (C4) does not appear to satisfy the linearity that is claimed in Theorem 1. However (C4) can be re-expressed in linear form and an optimal encoding is provided in Appendix B.

To illustrate the use of Theorem 1, consider a fixed network A that is equal to the complete network (exchangeable learning). Fig. 2 displays the MAP $\hat{G}^{(1:K)}|A$ computed (exactly) as a function of the regularity hyperparameter λ for a small fMRI dataset of 3 subjects containing measurements of activity in 4 neural regions. The first row, with $\lambda = 0$, is the result of performing independent estimation on the 3 subjects to obtain MAP estimators for subject-specific DAGs. Notice that the DAGs are quite dissimilar; the neuroscience context from which these data arise suggests that this is mainly an artefact of estimator variance. As the regularity parameter λ is increased, the subject-specific DAGs become increasingly similar until they are eventually identical at $\lambda = 0.3$ and above. In simulation studies below we demonstrate that exchangeable learning can lead to improved estimation of unit-specific graphical structure.

3.2 Exact Estimation of Multiple DAGs When A is Unknown

The previous section addressed the case where the interdependency structure A among units was known. In section 3.2.1 below we formulate an ILP for the more general case where A is unknown and must be estimated jointly with the unit-specific DAGs. In section 3.2.2 we show how this approach can be extended to include latent DAGs that induce group and subgroup structure between units. This allows us to formulate a novel analogue of k -means clustering for DAGs that may be useful for dimensionality reduction or in exploratory data analysis. We prove that BN mixture models are amenable as a special case of this procedure.

3.2.1 Exact Estimation of $G^{(1:K)}$ and A

In order to formulate an ILP in this extended setting we introduce additional binary indicator variables that directly encode which edges are present in the network A :

$$E^{(k,l)} := [(k, l) \in A] \quad \forall k, l \text{ with } k < l \quad (15)$$

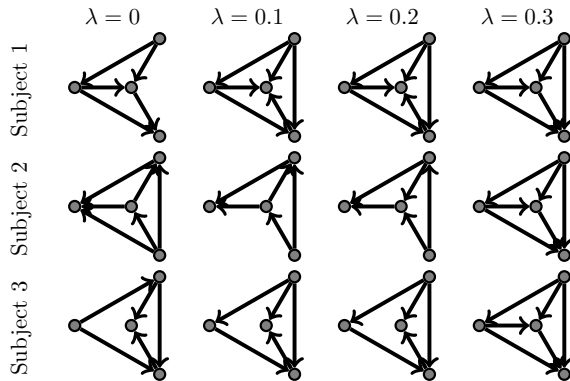


Figure 2: Illustration of exchangeable learning: A small fMRI dataset was obtained from 3 subjects, consisting of measurements of activity at 4 brain regions. Structure learning was performed using the proposed model for multiple DAGs with regularity parameter λ . Here we display the MAP estimator $\hat{G}^{(1:3)}|A$, where A is the complete network, for varying $\lambda \in \{0, 0.1, 0.2, 0.3\}$. For increasing λ we observe that the DAGs become progressively more similar.

Taking together the variables $d^{(k,l)}(j, i)$ and $E^{(k,l)}$ defined above allows us to determine whether or not an edge (j, i) differs between an unit k and its neighbour l in A . Specifically, we encode this information as

$$D^{(k,l)}(j, i) := [(j \in G_i^{(k)}) \oplus (j \in G_i^{(l)})] \& ((k, l) \in A) \quad \forall i, j, k, l \quad (\text{C5})$$

where $\&$ is the logical AND operator.

Theorem 2. *The MAP estimate $(\hat{G}^{(1:K)}, \hat{A})$ is characterised as the solution of the ILP*

$$\begin{aligned} (\hat{G}^{(1:K)}, \hat{A}) := \arg \max_{\substack{G^{(1:K)} \in \mathcal{G}^K \\ A \in \mathcal{A}}} & \sum_{k=1}^K \sum_{i=1}^P \sum_{\pi \subseteq \{1:P\} \setminus \{i\}} s^{(k)}(i, \pi) \Pi^{(k)}(i, \pi) \\ & - \lambda \sum_{i=1}^P \sum_{j=1}^P \sum_{k=1}^K \sum_{l=k+1}^K D^{(k,l)}(j, i) + \eta \sum_{k=1}^K \sum_{l=k+1}^K E^{(k,l)} \end{aligned} \quad (16)$$

subject to constraints (C1-5).

As before, although constraint (C5) is not linear, it is possible to re-express the constraint in linear form and an optimal encoding is provided in Appendix B.

3.2.2 k -Means Clustering of DAGs

Below we extend the ILP approach to accommodate latent units. Specifically, in addition to units $1 : K$ on which we observed data, we now introduce graphical models $G^{(K+1:K+L)}$. These latent units are really “doubly latent” in the sense that neither they, nor data directly conditional upon them, are observed. Here we describe a novel technique for probabilistic clustering of graphical models based on DAGs. We follow existing literature on k -means clustering and refer to cluster means as “prototypes” (MacKay, 2003). Latent units $K + 1 : K + L$ correspond to these prototypes and we aim to partition units $1 : K$ into L clusters such that the posterior probability of the cluster assignment is maximised. Depending on the application, it may or may not be required that latent graphs are acyclic. In this paper the latent graphs are required to satisfy DAG constraints (C1-2).

We call a network A on the extended vertex set $1 : K + L$ a “ k -means clustering of DAGs” if (i) A contains no edges between vertices k, l whenever $k < l \leq K$ or $K + 1 \leq k < l$, and (ii) A contains precisely

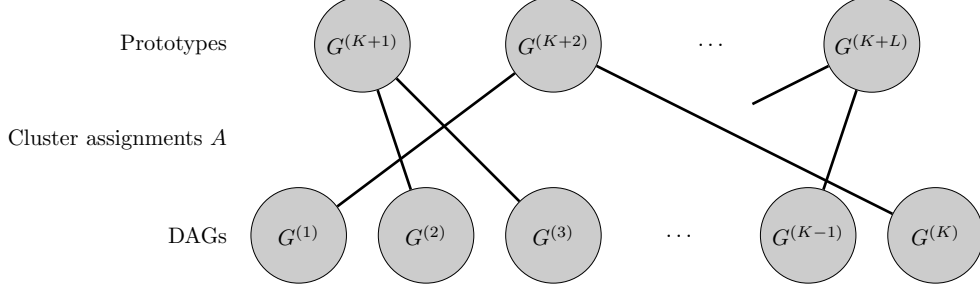


Figure 3: k -means clustering of DAGs. [Shaded nodes are unobserved and edges from DAGs to prototypes must be learned from data. $G^{(1:K)}$ = data-generating graphs, $G^{(K+1:L)}$ prototypes.]

one edge incident at each of the vertices k for $1 \leq k \leq K$. In other words, in a k -means clustering of DAGs, each network $G^{(1:K)}$ is joined by an edge to precisely one of the prototypes $G^{(K+1:K+L)}$ (Fig. 3). Units k, l connected to the same prototype are said to belong to the same “cluster” and we write $k \sim_C l$. Let $\mathcal{K}(L)$ be the set of all such clusterings based on L prototypes.

We introduce additional constraints (C6) $E^{(k,l)} = 0 \forall 1 \leq k, l \leq K$, (C7) $E^{(k,l)} = 0 \forall K+1 \leq k, l \leq K+L$ and (C8) $\sum_{l=K+1}^{K+L} E^{(k,l)} = 1 \forall 1 \leq k \leq K$. Here (C6) prohibits edges between data-generating DAGs, (C7) prohibits edges between prototypes, and (C8) ensures that each data-generating DAG is connected by an edge in A to precisely one of the prototypes.

Theorem 3. *The MAP estimate $(\hat{G}^{(1:K+L)}, \hat{A})$, conditional upon the network A belonging to $\mathcal{K}(L)$, is characterised as the solution of the ILP*

$$\begin{aligned}
 (\hat{G}^{(1:K+L)}, \hat{A}) := & \arg \max_{\substack{G^{(1:K+L)} \in \mathcal{G}^{K+L} \\ A \in \mathcal{A}}} \sum_{k=1}^K \sum_{i=1}^P \sum_{\pi \subseteq \{1:P\} \setminus \{i\}} s^{(k)}(i, \pi) \Pi^{(k)}(i, \pi) \\
 & - \lambda \sum_{i=1}^P \sum_{j=1}^P \sum_{k=1}^{K+L} \sum_{l=k+1}^{K+L} D^{(k,l)}(j, i)
 \end{aligned} \tag{17}$$

subject to constraints (C1-8).

Notice that each member of $\mathcal{K}(L)$ contains the same number of edges; it follows that $p(A)$ is uniform over $\mathcal{K}(L)$ and the ILP of Eqn. 17 is independent of the density hyperparameter η . Note also that, unlike classical k -means clustering (which typically involves stochastic optimisation and is not guaranteed to find a global maximum) the k -means clustering of DAGs we present here is an exact estimator. The components of the MAP corresponding to prototypes facilitate a convenient graphical summary of interplay for all members of the cluster and may be useful for dimensionality reduction.

Corollary 1. *For the ILP of Eqn. 17, there exists $\lambda^* \in [0, \infty)$ such that whenever $\lambda > \lambda^*$ we have that $k \sim_C l \implies G^{(k)} = G^{(l)}$.*

This result demonstrates that our statistical model is a strict generalisation of BN mixture models (Thiesson *et al.*, 1998), since for λ sufficiently large our estimates $\hat{G}^{(1:K)}$ can be grouped according to whether or not individual DAGs are identical. Moreover this opens up the previously unrecognised possibility of exploiting ILP methods for inference in BN mixture models.

4 Applications

We now investigate the statistical properties of the proposed estimators using both simulated data and data arising in a neuroscience context where joint modelling could be expected to achieve gains in estimation. Our

computational implementation is built on the C package GOBNILP that performs inference for individual DAGs (Bartlett and Cussens, 2013) and in Appendix B we summarise additional optimisation routines that underpin associated computational efficiency in the joint setting.

4.1 Simulation Study

In order to generate multiple related DAGs we employed a MCMC sampling scheme that targets the multiple DAG prior $p(G^{(1:K)}|A)$. Metropolis-Hastings proposals that switch the status (i.e. present or absent) of an edge (selected uniformly at random) within a unit (selected uniformly at random), subject to DAG constraints, achieved an average acceptance probability of 83%. Full pseudocode and convergence diagnostics are provided in the Supplement.

To generate the local scores $s^{(k)}(i, \pi)$ we appeal to the intuition that in many applications only a subset of models will be supported by data; we therefore generated scores independently according to the mixture model $\frac{100-\alpha}{100} \times \delta(-\infty) + \frac{\alpha}{100} \times N(0, 1)$, whilst the score of the true data-generating model is simulated from $N(0, 1)$. This ensures that the score of the data-generating model belongs to the top $\alpha\%$ of all scores, whilst allowing us to discard $(1 - \alpha)\%$ of all models and thereby reduce the computational burden in this simulation study. To further mediate computational complexity we imposed an in-degree restriction $d_{\max} = 2$ for all simulation experiments; this could be relaxed at additional computational effort. As the number P of variables increases, it is reasonable to increase the information present in the scores so that the inference problem does not become degenerate. We therefore set α adaptively, such that in each simulation the score associated with the true model belongs to the top P scores over all models.

The performance of structure learning algorithms for graphical models can be quantified in many ways (e.g. Peters and Bühlmann, 2014). In this paper we view estimation as a classification task whose samples correspond to individual edges; performance is then measured by the Matthews correlation coefficient (MCC) which is popular in scenarios where the number of negative samples (i.e. non-edges) can outweigh the number of positive samples (i.e. edges). All experiments below were repeated 10 times based on independently generated datasets. We emphasise that the multiple rounds of estimation performed in the simulation study below preclude comparison with more computationally intensive approaches such as Werhli and Husmeier (2008). On the other hand, methods that require a known and shared ordering of the variables such as Oates and Mukherjee (2014); Oyen and Lane (2013) do not apply in this general setting.

Exchangeable learning: Firstly we considered the case where the network A in the inference procedure is fixed equal to the complete network (exchangeable learning). We focussed on two distinct data-generating regimes: (i) The data-generating process has A complete with related but nonidentical DAGs, and (ii) the data-generating process has A as two disconnected complete components of equal size and DAGs that are identical within each component. Regime (i) employs exchangeable learning in a favourable setting where information is shared between all DAGs, whilst regime (ii) employs exchangeable learning in an unfavourable setting, where the assumption of exchangeability is most strongly violated. Results for regime (i) in Fig. 4 demonstrate that substantially improved performance is achieved by our joint estimators compared to independent estimation. We also see that inference based on $\lambda = \infty$, i.e. the estimator that requires all DAGs to have identical structure, performs worse in general than inference based on an appropriately selected regularity parameter λ , as expected. The same datasets were employed for each value of λ to ensure a fair comparison. Results from regime (ii) in Fig. ?? show that, despite the exchangeability assumption being strongly violated, exchangeable learning remains competitive with independent estimation, but inference that assigns the same DAG to all units performs extremely poorly, as expected.

Nonexchangeable learning: Secondly we considered the case where the network A is unknown and must be learned along with the individual networks $G^{(1:K)}$. In general the data-generating A could have any topology; we again focussed on the two distinct regimes described above. Regime (i) aims to examine the loss of statistical efficiency that results from employing nonexchangeable learning when exchangeable learning would be more suitable, whilst regime (ii) explores the challenging case where the unknown A is highly informative, so that the loss of information that comes from not knowing A is greatest. Results for regime (i) in Fig. 5(a-b) demonstrate that, despite being extremely general, nonexchangeable learning still achieves improved estimation compared to independent inference for most values of the hyperparameters

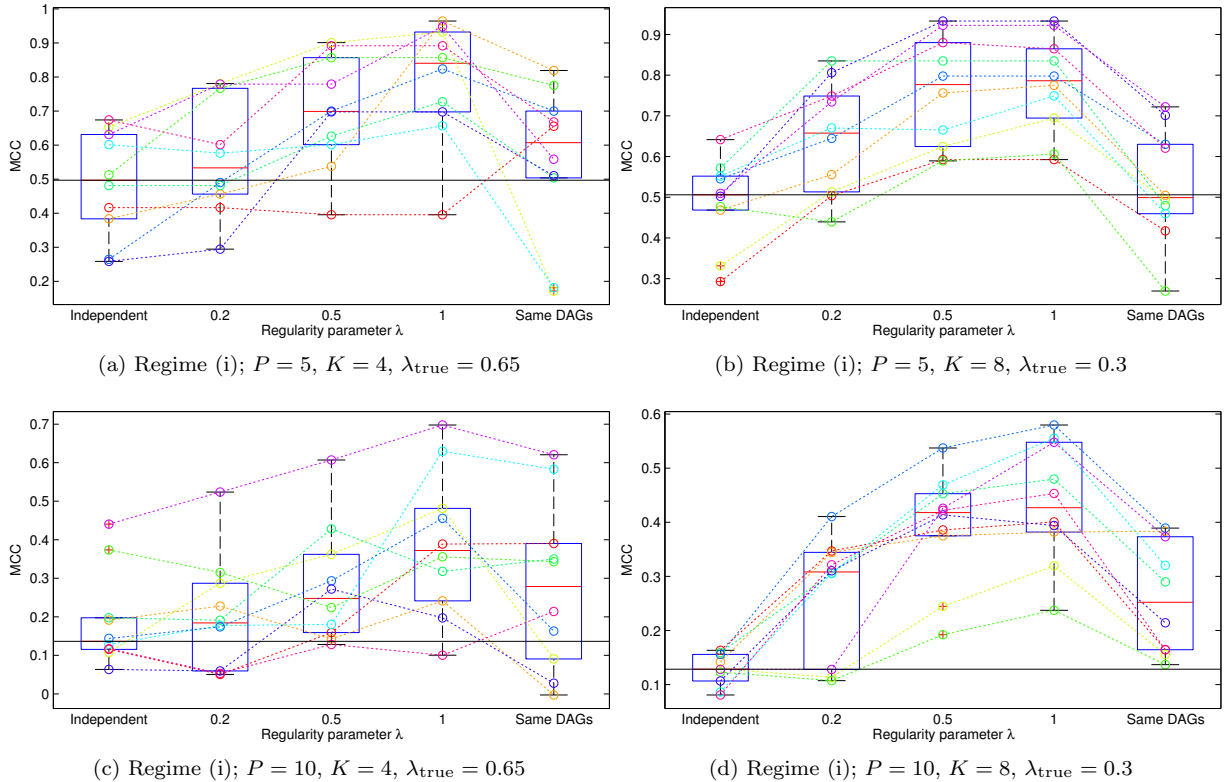


Figure 4: Exchangeable learning of multiple DAGs. [In regime (i) the data-generating DAGs satisfy an exchangeability assumption. Here P is the number of variables, K is the number of units, MCC is the Matthews correlation coefficient and λ_{true} is the data-generating regularity parameter. Horizontal lines are the median MCC achieved under independent inference. For fair comparison the same 10 datasets were subject to estimation using different values of the regularity parameter λ ; these are shown as dashed lines.]

λ, η that we considered. For regime (ii), shown in Fig. 5(c-d), we see that estimation is more challenging, as expected. For this regime it is also interesting to ask whether the network A that relates units is itself accurately estimated; Fig. ?? confirms that estimation of A appears to be challenging in this regime and explains why the performance of our estimators does not improve on independent estimation in this case.

k -means clustering of DAGs: Finally we examined the ability of our clustering procedure to infer latent class labels. Here we consider 2 clusters each containing 4 units and focus on two distinct regimes: (i) All DAGs within a cluster are identical, and (ii) DAGs within a cluster are related but are non-identical. Results in Fig. 6 demonstrate that, in regime (i), not only can the cluster assignments be accurately recovered but the individual DAGs themselves can be accurately estimated. Regime (ii) is more challenging but again we see gains from using joint estimation over independent estimation.

4.2 MDMs for Neural Activity in a Multi-Subject Study

We illustrate our methodology by analysing data generated from a functional magnetic resonance imaging (fMRI) experiment, designed to assess how one neural system influences another when a person remains in a state of quiet repose. It is typical for fMRI experiments to involve multiple subjects; data analysis should therefore take into account not only the interaction between areas of one brain but also the similarities and differences among subjects (Mechelli *et al.*, 2002). For instance, Sugihara *et al.* (2006) showed that the communication pattern among brain regions may be subject-specific, using a fMRI data derived from a

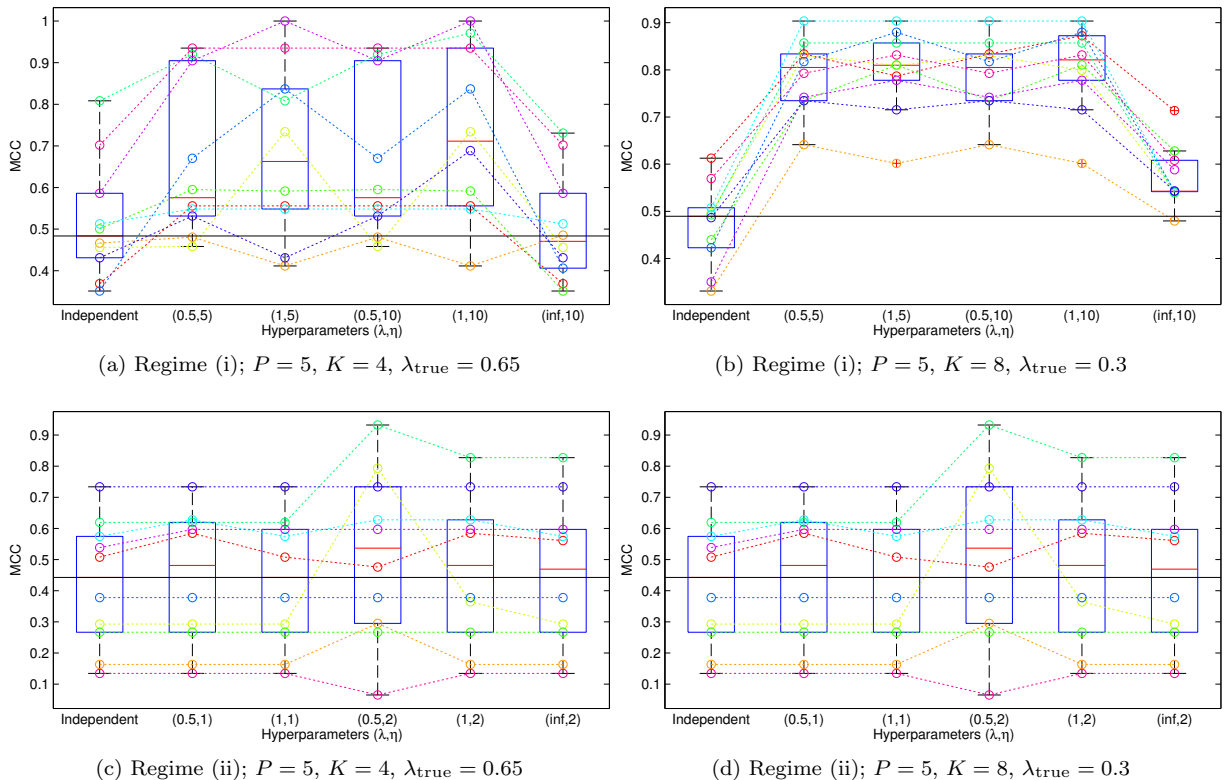


Figure 5: Nonexchangeable learning of multiple DAGs. [In regime (i) the data-generating DAGs satisfy an exchangeability assumption, whereas in regime (ii) the data-generating DAGs strongly violate exchangeability (see Main Text for details). Here P is the number of variables, K is the number of units, MCC is the Matthews correlation coefficient and λ_{true} is the data-generating regularity parameter. Horizontal lines are the median MCC achieved under independent inference. For fair comparison the same 10 datasets were subject to estimation using different values of the hyperparameters (λ, η) ; these are shown as dashed lines.]

writing experiment, whilst (Li *et al.*, 2008) argue that the causal relations between brain regions can vary in disease states according to the severity of the disease. Given that the mechanisms underpinning subject-specific variation are largely unknown, the statistical elicitation of subject-specific connectivity patterns in a multi-subject study is central to the scientific investigation of neural signalling.

The interactions (or connections) among different cerebral areas are usually studied through causal DAG models (Friston, 2011; Poldrack *et al.*, 2011). Here we are using the multiregression dynamical model (MDM) for fMRI data developed by Costa *et al.* (2013), in which edges denote direct contemporaneous relationships that might exist between nodes and the connections are represented by parameters that vary over time, thereby generalising classical “static” BNs. Costa *et al.* (2013) provide a search process, for individual MDMs, based on ILP. There it was shown that MDMs were capable of detecting the presence of connections between brain regions and also discerning the directionality of these connections. Our present work extend this methodology to the scientifically important case of comparison between multiple subjects. The specific application below is discussed in greater detail from an applied statistical perspective in Oates *et al.* (2014).

The MDM is defined on a multivariate time series that aims to identify the causal structure among the variables over time (Queen and Smith, 1993; Queen and Albers, 2009). In the MDM that we consider, a multivariate model for observable series $\mathbf{Y}^{(k)}(n)$, for subject k at time n is characterised by a contemporaneous DAG, with information shared across time only through evolution of the model parameters $\theta_i^{(k)}(n)$.

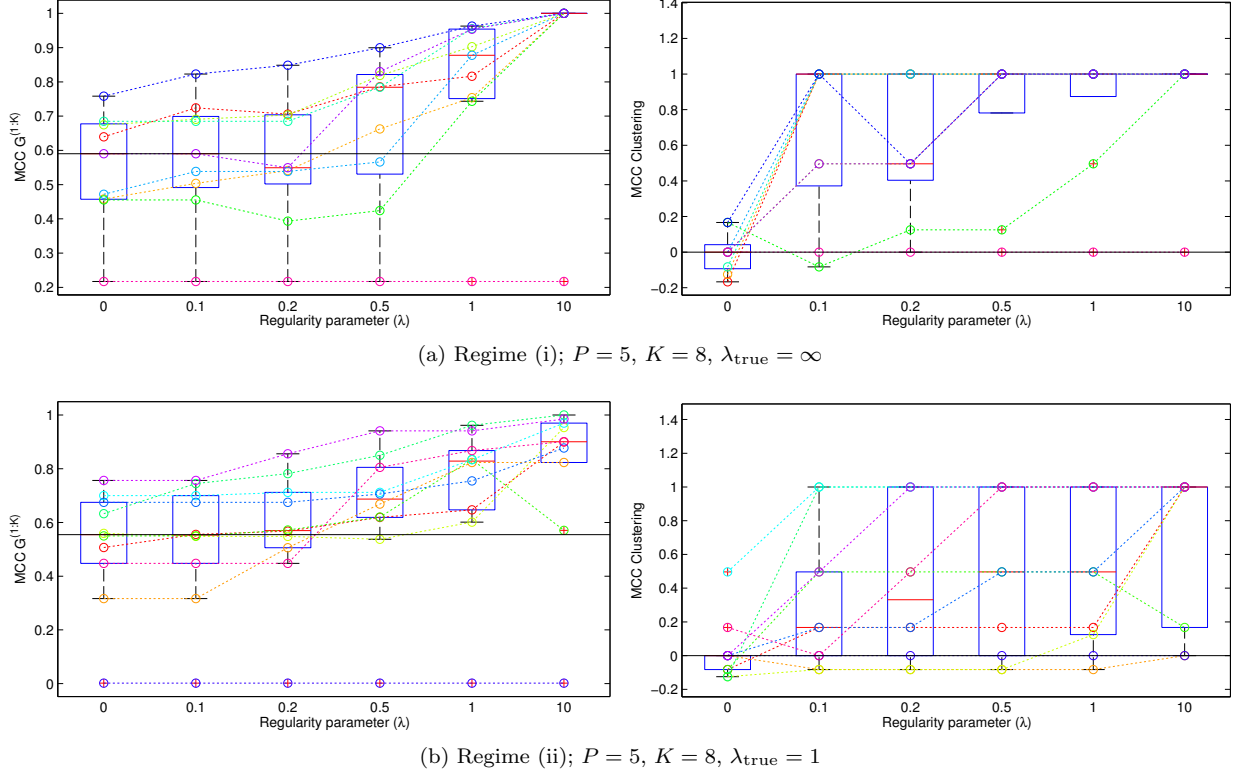


Figure 6: k -means clustering of DAGs: In regime (i) data were generated from 2 clusters each containing 4 units, such that units belonging to the same cluster share the same DAG structure. In regime (ii) the structure of DAGs within a cluster is permitted to vary. [Here P is the number of variables, K is the number of units, MCC is the Matthews correlation coefficient and λ_{true} is the data-generating regularity parameter. Horizontal lines are the median MCC achieved under independent inference. For fair comparison the same 10 datasets were subject to estimation using different values of the regularity parameter λ ; these are shown as dashed lines.]

This was the setting considered in Costa *et al.* (2013), however the framework we propose applies equally to MDMs that permit edges connecting variables through time (see Queen and Smith, 1993). We further consider the simplest case where $\mathbf{Y}^{(k)}(n)|\boldsymbol{\theta}^{(k)}(n)$ satisfies linear Gaussian structural equations, though our methodology does not dictate how the local models are specified. Formally, this model is described by the following observation equations and system equations:

$$Y_i^{(k)}(n) = \mathbf{Y}_{G_i^{(k)}}^{(k)}(n)^T \boldsymbol{\theta}_i^{(k)}(n) + \epsilon_i^{(k)}(n), \quad \epsilon_i^{(k)}(n) \sim N(0, V_i^{(k)}(n)) \quad (18)$$

$$\boldsymbol{\theta}^{(k)}(n) = \boldsymbol{\Gamma}^{(k)}(n) \boldsymbol{\theta}^{(k)}(n-1) + \mathbf{w}^{(k)}(n), \quad \mathbf{w}^{(k)}(n) \sim N(\mathbf{0}, \mathbf{W}^{(k)}(n)) \quad (19)$$

where $\boldsymbol{\theta}^{(k)}(n)^T = (\boldsymbol{\theta}_1^{(k)}(n)^T, \dots, \boldsymbol{\theta}_P^{(k)}(n)^T)$ is the concatenated parameter vector and $V_i^{(k)}(n)$, $\boldsymbol{\Gamma}^{(k)}(n)$, $\mathbf{W}^{(k)}(n)$ must be specified. The equations of the MDM can be viewed as a collection of nested univariate linear models, allowing the parameters to be estimated using well-known Kalman Filter recurrences over time.

One of the most popular approaches to model selection in this setting is based on Bayes factors (see e.g. West and Harrison, 1997). The evidence in favour of the DAG $G^{(k)}$ under the MDM likelihood can be

calculated as

$$p(\mathbf{Y}^{(k)}|G^{(k)}) = \prod_{i=1}^P \prod_{n=1}^N p(Y_i^{(k)}(n)|\mathbf{Y}_{G_i^{(k)}}^{(k)}(n), \mathbf{Y}^{(k)}(1:n-1), G_i^{(k)}),$$

where $\mathbf{Y}^{(k)}(1:n-1) = (\mathbf{Y}^{(k)}(1), \dots, \mathbf{Y}^{(k)}(n-1))$ is the collection of observed values from subject k up until time $n-1$. Under the conjugate formulation of Costa *et al.* (2013), the conditional forecast distribution on the right hand side of Eqn. 20 has the closed form of a student’s t -distribution. We refer the reader to Costa *et al.* (2013) for further details regarding prior elicitation and construction of Bayes factors in this setting.

Our methodology is illustrated here with a small fMRI dataset consisting of six unrelated subjects from the Human Connectome Project (Van Essen *et al.*, 2013). Data were acquired on each subject while they were in a state of quiet repose and preprocessed to obtain 10-dimensional time series representing the activity levels at 10 regions in each subject. Full details are provided in the accompanying paper Oates *et al.* (2014).

The graphical structures obtained using independent estimation applied to the 6 subjects, shown in Fig. 7 (top), are unsatisfactory on biological grounds since it is anticipated that connectivity does not change substantially between subjects. On the other hand it is expected that graphical structures corresponding to different subjects are likely to be non-identical, due to the ill-posed notion of a “resting state” (Ringach, 2009), so that pooling datasets together in a naive fashion would be inappropriate, and even suppress scientifically interesting subject-specific connectivity. This motivates a unified statistical framework for multiple DAGs and the use of the exact estimators introduced above.

Exchangeable learning: We began by inferring DAGs $G^{(1:K)}$ under an exchangeability assumption, for various values of the regularity hyperparameter λ (Fig. 7). Elicitation of an appropriate value for λ can be achieved in this setting by exploiting technical replicate data and examination of Bayes factors, as discussed at length in Oates *et al.* (2014). For this dataset and the subsequent analysis we elicited $\lambda = 4$.

Nonexchangeable learning: Based on $\lambda = 4$ we then performed nonexchangeable learning in order to estimate similarities and differences between the 6 subjects in terms of their neural connectivity. Specifically, we estimate a network A on these 6 subjects, based on various values of the density hyperparameter η . Results, shown in Fig. 8, indicate that at $\eta = 60$, subjects 1 and 4, 2 and 3, and 5 and 6 exhibit the most similar graphical structures. Non-edges $(k, l) \notin A$ in the network A are indicative of differences in the graphical structure; such information may therefore be used to identify subjects with particularly aberrant connectivity for further scientific investigation. Going further, we see that subjects 5 and 6 are perhaps the most unusual, being totally disconnected from subjects 1 to 4 in the network A when $\eta = 70$. If required, elicitation of η can proceed based on Bayes factors as discussed in Oates *et al.* (2014).

k -means clustering of DAGs: Finally we applied k -means clustering of DAGs with both $L = 2$ and $L = 3$ mixture components. Results show that for $L = 2$ (Fig. ??) we obtain clusters $\{1, 2, 3\}$, $\{4, 5, 6\}$, and for $L = 3$ (Fig. ??) we obtain clusters $\{1, 4\}$, $\{2, 3\}$, $\{5, 6\}$. This accords with the network A obtained at $\eta = 60$, in the sense that mixture components correspond exactly to connected components. Thus k -means clustering could provide an alternative to nonexchangeable learning when the goal is to estimate the extent to which units display similar structure.

Further interpretation of these results is reserved for Oates *et al.* (2014).

5 Discussion

This paper introduced a general statistical framework for multiple DAGs that are regularised based on graphical structure and proved that several MAP estimates are characterised as the solutions to ILPs, hence admitting efficient exact algorithms. We believe these to be the first exact algorithms for the general case of multiple DAG models. In addition to a general framework for joint learning, we allowed for a complex dependence structure on the collection of units that considerably generalises existing exchangeable models. Results obtained both from simulations and from an application in neuroscience demonstrate that joint estimation of DAGs can increase statistical efficiency relative to independent estimation. Through the neuroscience application we showed how sophisticated likelihood models such as MDMs may be integrated

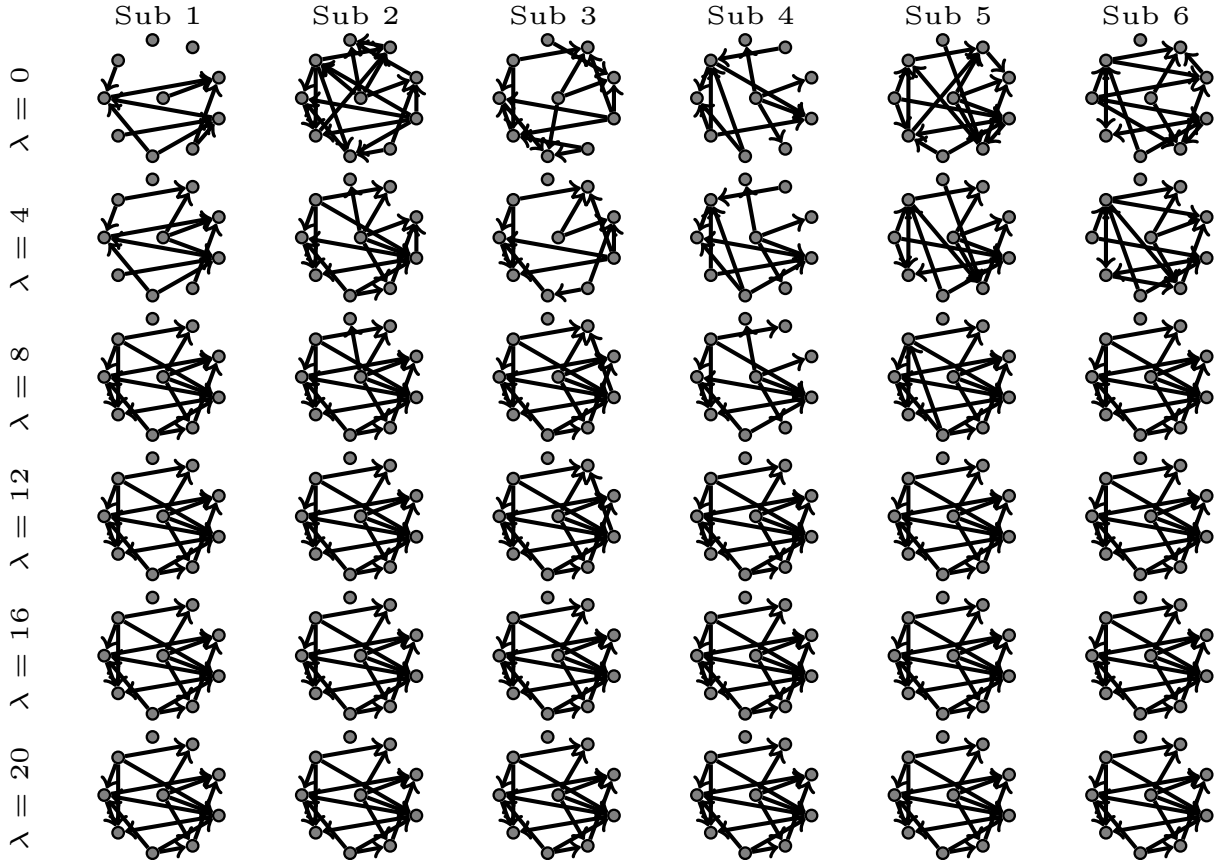


Figure 7: Neuroscience data; exchangeable learning. [Here we simultaneously estimate subject-specific DAGs for different values of the regularity hyperparameter λ .]

into our framework. Importantly, our methodology requires only that local scores are pre-computed and cached; it is therefore possible to apply exact algorithms retrospectively, following unsatisfactory independent analyses of individual datasets, without the need to recompute model scores. In practice we anticipate that the rationale and appropriateness of joint modelling will need be assessed by domain-experts on a case-by-case basis.

Our computations were performed using the GOBNILP package (Bartlett and Cussens, 2013), which includes sophisticated routines for estimation of individual DAGs (see Appendix B). Nevertheless our simulation results for large numbers P of variables and K of units required considerable computational time, since in general for nonexchangeable learning the number of constraints required increases as $\mathcal{O}(P^2K^2)$. It is becoming commonplace in many applications for the number of units to become very large. It remains to be seen whether our method could cope with such numbers. Recent work `nuala` where GOBNILP was able to find MAP DAGs with 1614 nodes in between 3 and 42 minutes offers some hope that it will (Sheehan *et al.*, 2014). In practice, as discussed in Bartlett and Cussens (2013), it is very hard to estimate the time required to solve an ILP in advance; rather this depends in a highly non-trivial way on the details of the problem, and is related to the “phase-transition” in SAT solving.

We note that the results of this paper are based on the ILP framework of Jaakola *et al.* (2010) for individual DAGs. An alternative ILP formulation, known as “characteristic imsets”, was proposed by Studený *et al.* (2010) specifically for BNs. Characteristic imsets are closely related to the “essential graph” of a BN (Pearl, 2009) and have the property that Markov-equivalent BNs are score equivalent. In contrast, the approaches

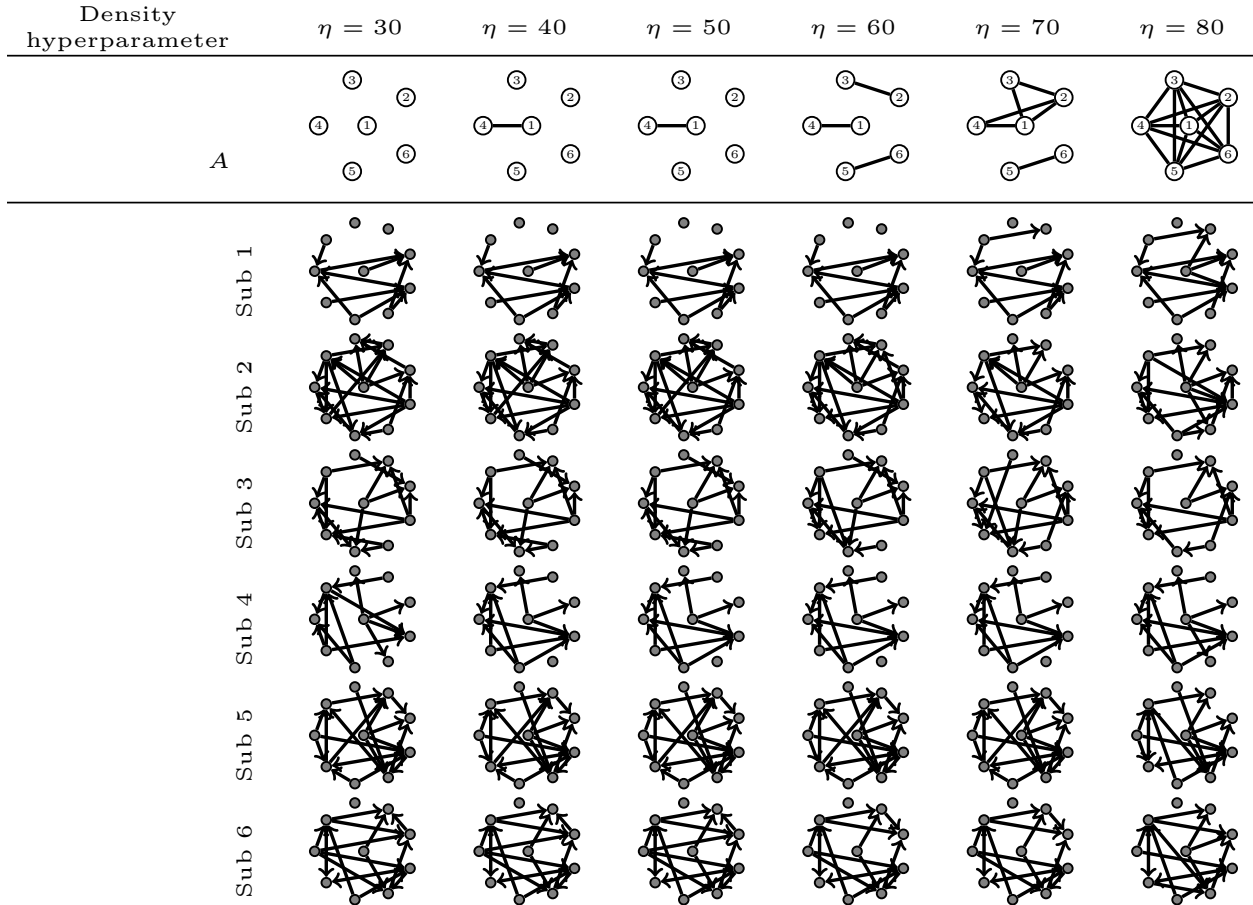


Figure 8: Neuroscience data; nonexchangeable learning. [Here we simultaneously estimate both subject-specific DAGs and the network A that relates subjects. The regularity hyperparameter $\lambda = 4$ was fixed whilst the density hyperparameter η was varied.]

we pursue involve a non-unique representation of the essential graph. This flexibility is important when dealing with general DAG models including MDMs, that are uniquely identifiable from data. At present, the computational performance of characteristic insets on individual BNs is inferior to the approach of Jaakola *et al.* (2010) pursued here (Studený and Haws, 2013). In addition it is currently unclear how prior structural information might be incorporated into this framework.

Interesting theoretical extensions that relate directly to the case of multiple DAGs include:

1. **Information sharing for parameters.** In many applications it is reasonable to assume prior similarity of parameter values between units. At present this appears to be challenging to include within our framework, and represents an interesting area for further research.
2. **Elicitation.** Strategies for hyperparameter elicitation are discussed in Oates *et al.* (2014), but in general this procedure will be application-specific. It is important to note that “robust” estimation is somewhat orthogonal to the challenge of performing inferences about the data-generating process. In applications where the local likelihood model is misspecified, the techniques discussed here may produce more robust estimators, but that robustness may be artefactual and not due to a gain in statistical efficiency. The problem of elicitation therefore also includes assessment of the appropriateness of the likelihood model on a case-by-case basis.

3. **Computation.** The applications discussed in this paper were performed on a single CPU and limited in computational intensity to approximately $P, K \leq 10$. Since many emerging datasets, particularly in disease genomics, contain many more variables P and many more units K than we considered here, it would be interesting to investigate strategies for parallel and/or approximate computation that scale better to such regimes. In the other direction, our methodology applies to complex local scores which may be estimated numerically; it would be interesting to gain a theoretical understanding of how uncertainty in the estimates for the local scores impacts on the MAP estimators described here.

Acknowledgements

CJO was supported by the Centre for Research in Statistical Methodology (CRiSM) EPSRC EP/D002060/1. JC was supported by the Medical Research Council (Project Grant G1002312). The authors are grateful to Lilia Carneiro da Costa and Tom Nichols who collaborated in the analysis of fMRI data and to Mark Bartlett who provided technical support with GOBNILP.

Appendix A

Theorem 1. We begin by showing that the objective function is equal to the log-posterior density (up to an additive constant):

$$\log(p(G^{(1:K)} | \mathbf{Y}^{(1:K)}, A)) \stackrel{+C}{=} \log(p(\mathbf{Y}^{(1:K)} | G^{(1:K)})) + \log(p(G^{(1:K)} | A)) \quad (20)$$

$$\stackrel{+C}{=} \sum_{k=1}^K \sum_{i=1}^P \log(p(\mathbf{Y}_i^{(k)} | \mathbf{Y}_{G_i^{(k)}}^{(k)}, G_i^{(k)})) \\ + \sum_{(k,l) \in A} \log(r(G^{(k)}, G^{(l)})) + \sum_{k=1}^K \sum_{i=1}^P \log(m_i(G_i^{(k)})) \quad (21)$$

$$= \sum_{k=1}^K \sum_{i=1}^P s^{(k)}(i, G_i^{(k)}) + \sum_{(k,l) \in A} \log(r(G^{(k)}, G^{(l)})) \quad (22)$$

where Eqn. 21 follows from Eqn. 2 and Eqn. 22 follows from the definition of the local scores $s^{(k)}(i, G_i^{(k)})$. Now (C4) implies that $\sum_{i=1}^P \sum_{j=1}^P d^{(k,l)}(j, i)$ counts the number of edges that differ between $G^{(k)}$ and $G^{(l)}$. Thus under SHD we have the equality

$$= \sum_{k=1}^K \sum_{i=1}^P \sum_{\pi \subseteq \{1:P\} \setminus \{i\}} s^{(k)}(i, G_i^{(k)}) [G_i^{(k)} = \pi] - \lambda \sum_{(k,l) \in A} \sum_{i=1}^P \sum_{j=1}^P d^{(k,l)}(j, i) \quad (23)$$

which is seen to be the basis for the ILP in Eqn. 14. It remains to show that constraints (C1) and (C2) ensure that the $G^{(1:K)}$ that satisfy them are precisely the set \mathcal{G}^K of all possible combinations of DAGs; this final step is proved in Jaakola *et al.* (2010). \square

Theorem 2. We again begin by showing that the objective function is equal to the log-posterior (up to an additive constant):

$$\log[= (p(G^{(1:K)}, A | \mathbf{Y}^{(1:K)})) \stackrel{+C}{=} \log(p(\mathbf{Y}^{(1:K)} | G^{(1:K)})) + \log(p(G^{(1:K)} | A)) + \log(p(A)) \quad (24) \\ \stackrel{+C}{=} \sum_{k=1}^K \sum_{i=1}^P s^{(k)}(i, G_i^{(k)}) + \sum_{(k,l) \in A} \log(r(G^{(k)}, G^{(l)})) + \log(p(A)).$$

Then since $E^{(k,l)} = 1$ if $(k, l) \in A$ and zero otherwise and from the definition of $p(A)$, we have

$$= \sum_{k=1}^K \sum_{i=1}^P s^{(k)}(i, G_i^{(k)}) - \lambda \sum_{k=1}^K \sum_{l=k+1}^K E^{(k,l)} \sum_{i=1}^P \sum_{j=1}^P d^{(k,l)}(j, i) + \eta \sum_{k=1}^K \sum_{l=k+1}^K E^{(k,l)} \quad (25)$$

$$= \sum_{k=1}^K \sum_{i=1}^P s^{(k)}(i, G_i^{(k)}) \Pi^{(k)}(i, G_i^{(k)}) - \lambda \sum_{i=1}^P \sum_{j=1}^P \sum_{k=1}^K \sum_{l=k+1}^K D^{(k,l)}(j, i) + \eta \sum_{k=1}^K \sum_{l=k+1}^K E^{(k,l)}. \quad (26)$$

Here the final line follows from (C5) since $D^{(k,l)}(j, i) = 1$ if both $(k, l) \in A$ and $(j \in G_i^{(k)}) \oplus (j \in G_i^{(l)})$ and zero otherwise. Again, the results of Jaakola *et al.* (2010) complete the argument by ensuring (C1-2) characterise the set \mathcal{G} of DAGs. \square

Theorem 3. This follows immediately from Theorem 2 and the observation that (C6-8) characterise a k -means clustering of DAGs. \square

Appendix B

The computations for this paper were performed using GOBNILP, available at <http://www.cs.york.ac.uk/aig/sw/gobnilp/>. GOBNILP, originally described in Cussens (2011), computes the MAP estimate on a per-unit basis; we therefore created an interface that interacts with GOBNILP and enforces additional constraints that couple together multiple DAGs as described above. Below we elaborate on how such an interface was constructed.

Since there are exponentially many acyclicity constraints (C2), GOBNILP does *not* construct an integer program (IP) containing all of them. Instead, initially, only the convexity constraints (C1) are included in an IP. GOBNILP then (exactly) solves the linear program (LP) relaxation of the IP where integer variables are (temporarily) allowed to take any real value within their bounds. (In practice GOBNILP employs an LP solver such as SOPLEX or CPLEX to do this task.) This produces an LP solution \mathbf{x}^* . Crucially, the LP solution can be found very quickly. GOBNILP then searches for (C2) acyclicity constraints that \mathbf{x}^* violates and adds them to the IP. Linear constraints added in this way are known as ‘cutting planes’ since they ‘cut off’ the infeasible solution \mathbf{x}^* . GOBNILP then solves the linear relaxation of this new IP and looks for cutting planes for the new LP solution. This process of solving linear relaxations and adding cutting planes is then repeated. Note that the sequence of LP solutions produced in this way provide increasingly tight upper bounds on the objective value of an optimal DAG.

It can happen that an LP solution represents a DAG (i.e. all variables have integer values and the graph they represent is acyclic). In this case, the problem is solved exactly, since any LP solution provides an upper bound on the objective function. More typically (at least on larger problems) a fractional LP solution is generated that satisfies all acyclicity constraints. In such a situation GOBNILP selects a fractional variable $\Pi(i, \pi)$ to branch on, creating two subproblems, one where $\Pi(i, \pi) = 0$ (ruling out parent set π for variable i) and one where $\Pi(i, \pi) = 1$ (setting the parent set of variable i to be π). The GOBNILP algorithm is then applied recursively on both branches. When an IP variable $\Pi(i, \pi)$ is set to 1, GOBNILP performs ‘propagation’ and sets to 0 those IP variables which indicate other parent sets for i or parent set choices for other variables that are no longer possible under the acyclicity constraint.

This approach to IP solving is known as ‘branch-and-cut’ since both branching on variables and adding cutting planes are used. GOBNILP is implemented using the SCIP framework due to Achterberg (2009). The basic GOBNILP algorithm described above has been optimised in a number of ways: e.g. extra linear constraints are added to the initial IP and additional cutting plane algorithms (some built into SCIP, some GOBNILP-specific) are used. In addition, a heuristic algorithm (based on ‘rounding’ the current LP solution) is used to generate ‘good’ but probably sub-optimal DAGs. This can help prune the search tree produced by branching on variables. See (Bartlett and Cussens, 2013) for further details.

For this work we constructed an interface for GOBNILP that interlaces with SCIP to include additional constraints that couple together estimation problems for multiple DAGs. To achieve this it is necessary to

express the constraints (C4-5) in linear form. To encode (C4) we use the set of linear inequalities

$$+d^{(k,l)}(j, i) \quad -e^{(k)}(j, i) \quad -e^{(l)}(j, i) \quad \leq \quad 0 \quad (27)$$

$$-d^{(k,l)}(j, i) \quad +e^{(k)}(j, i) \quad -e^{(l)}(j, i) \quad \leq \quad 0 \quad (28)$$

$$-d^{(k,l)}(j, i) \quad -e^{(k)}(j, i) \quad +e^{(l)}(j, i) \quad \leq \quad 0 \quad (29)$$

$$+d^{(k,l)}(j, i) \quad +e^{(k)}(j, i) \quad +e^{(l)}(j, i) \quad \leq \quad 2 \quad (30)$$

In practice these are implemented using SCIP’s XOR constraint handler. This handles any constraint of the form $r = x_1 \oplus x_2 \oplus \dots \oplus x_n$ where $r, x_i \in \{0, 1\}$ and the constraint is satisfied if either $r = 1$ and an odd number of the x_i are 1, or $r = 0$ and an even number of the x_i are 0. We set $0 = d^{(k,l)}(j, i) \oplus e^{(k)}(j, i) \oplus e^{(l)}(j, i)$. The linear inequalities (27-30) are optimal in the sense that they define the convex hull (in \mathbb{R}^3) of feasible solutions to our 3-variable XOR constraint (Achterberg, 2007). In practice SCIP generates these inequalities internally and also provides a propagator for XOR constraints; in the simplest case, as soon as any two of $d^{(k,l)}(j, i)$, $e^{(k)}(j, i)$ and $e^{(l)}(j, i)$ have their values fixed then SCIP will immediately fixed the value of the third appropriately. Similarly, to encode (C5) we use the set of linear inequalities

$$+D^{(k,l)}(j, i) \quad -E^{(k,l)} \quad \leq \quad 0 \quad (31)$$

$$+D^{(k,l)}(j, i) \quad -d^{(k,l)}(j, i) \quad \leq \quad 0 \quad (32)$$

$$-D^{(k,l)}(j, i) \quad +E^{(k,l)} \quad +d^{(k,l)}(j, i) \quad \leq \quad 1. \quad (33)$$

In practice these are implemented using SCIP’s AND constraint handler. This handles any constraint of the form $r = x_1 \& x_2 \& \dots \& x_n$, where $r, x_i \in \{0, 1\}$. We set $D^{(k,l)}(j, i) = E^{(k,l)} \& d^{(k,l)}(j, i)$. The linear inequalities (31-33) are internally generated by SCIP and again define the convex hull of feasible solutions (Achterberg, 2007). SCIP provides a propagator for AND constraints which works analogously to that for XOR constraints.

In this paper we restrict attention to the MAP estimator, but the GOBNILP software and our interface facilitate the efficient computation of the “top n ” solutions to the ILP corresponding to the n best joint estimates of DAG structure, along with their associated values for the objective function (and hence Bayes factors). The interfacing software is written for MATLAB R2014a and is provided in the Supplement.

References

- Acid, S., de Campos, L.M. (2003) Searching for Bayesian network structures in the space of restricted acyclic partially directed graphs. *J. Artif. Intell. Res.* **18**:445-490.
- Achterberg, T. (2007). *Constraint integer programming*. PhD Thesis, Berlin Institute of Technology.
- Achterberg, T. (2009). SCIP: solving constraint integer programs. *Mathematical Programming Computation* **1**(1):1-41.
- Bartlett, M., Cussens, J. (2013) Advances in Bayesian Network Learning using Integer Programming. *Proceedings of the 29th Conference on Uncertainty in Artificial Intelligence*: 182-191.
- Barretina *et al.* (2012) The Cancer Cell Line Encyclopedia enables predictive modelling of anticancer drug sensitivity. *Nature* **483**(7391):603-607.
- Baumbach *et al.* (2009) Reliable transfer of gene regulatory networks between taxonomically related organisms. *BMC Bioinformatics* **3**(1):8.
- Boutilier *et al.* (1996) Context-specific independence in Bayesian networks. *Proceedings of the 12th Annual Conference on Uncertainty in Artificial Intelligence*: 115-123.

- Bowsher, C.G. (2010) Stochastic Kinetic Models: Dynamic Independence, Modularity and Graphs. *Ann. Stat.* **38**(4):2242-2281.
- Cao *et al.* (2011) Whole-genome sequencing of multiple *Arabidopsis thaliana* populations. *Nat. Genet.* **43**(10):956-963.
- Chandrasekaran, V., Parrilo, P.A., Willsky, A.S. (2012) Latent Variable Graphical Model Selection via Convex Optimisation. *Ann. Stat.* **40**(4):1935-1967.
- Chiquet, J., Grandvalet, Y., Ambroise, C. (2011). Inferring multiple graphical structures. *Stat. Comput.* **21**(4):537-553.
- Claassen, T., Heskes, T. (2012) A Bayesian Approach to Constraint Based Causal Inference. *Proceedings of the 28th Conference on Uncertainty in Artificial Intelligence*: 207-216.
- Consonni, G., La Rocca, L. (2010) Moment Priors for Bayesian Model Choice with Applications to Directed Acyclic Graphs. *Bayesian Statistics* **9**(9):119-144.
- Costa, L., Smith, J.Q., Nicholls, T. (2013) On the selection of Multiregression Dynamic Models of fMRI networked time series. *CRiSM Working Paper, University of Warwick* **13**:6.
- Cowell, R.G. (2009) Efficient maximum likelihood pedigree reconstruction. *Theor. Popul. Biol.* **76**:285-291.
- Csermely *et al.* (2013) Structure and dynamics of molecular networks: A novel paradigm of drug discovery: A comprehensive review. *Pharmacol. Therapeut.* **138**(3):333-408.
- Curtis *et al.* (2012) The genomic and transcriptomic architecture of 2,000 breast tumours reveals novel subgroups, *Nature* **486**(7403):346-352.
- Cussens, J. (2010) Maximum likelihood pedigree reconstruction using integer programming. *Proceedings of the Workshop on Constraint Based Methods for Bioinformatics (WCB-10), Edinburgh*.
- Cussens, J. (2011) Bayesian network learning with cutting planes. *Proceedings of the 27th Conference on Uncertainty in Artificial Intelligence*: 153-160.
- Danaher, P., Wang, P., Witten, D.M. (2014) The joint graphical lasso for inverse covariance estimation across multiple classes. *J. R. Statist. Soc. B* **76**(2):373-397.
- Dawid, A.P., Lauritzen, S.L. (1993) Hyper Markov laws in the statistical analysis of decomposable graphical models. *Ann. Stat.* **21**(3):1272-1317.
- Ellis, B., Wong, W.H. (2008) Learning Causal Bayesian Network Structures From Experimental Data. *J. Am. Stat. Assoc.* **103**(482):778-789.
- Friedman, N., Koller, D. (2003) Being Bayesian about Network Structure: A Bayesian Approach to Structure Discovery in Bayesian Networks. *Mach. Learn.* **50**(1-2):95-126.
- Friston, K.J. (2011) Functional and Effective Connectivity: A review. *Brain Connectivity* **1**(1):13-36.
- Geiger, D., Heckerman, D. (1996) Knowledge representation and inference in similarity networks and Bayesian multinets. *Artif. Intell.* **82**(1):45-74.
- Hara, S., Washio, T. (2012) Learning a common substructure of multiple graphical Gaussian models. *Neural Networks* **38**:23-38.
- He, Y., Jia, J., Yu, B. (2013) Reversible MCMC on Markov equivalence classes of sparse directed acyclic graphs. *Ann. Stat.* **41**(4):1742-1779.

- Heckerman, D., Geiger, D., Chickering, D.M. (1995) Learning Bayesian networks: The combination of knowledge and statistical data. *Mach. Learn.* **20**(3):197-243.
- Hill *et al.* (2012) Bayesian Inference of Signaling Network Topology in a Cancer Cell Line. *Bioinformatics* **28**(21):2804-2810.
- Ideker, T., Krogan, N.J. (2012) Differential network biology. *Mol. Syst. Biol.* **8**(1):565.
- Jaakkola *et al.* (2010) Learning Bayesian network structure using LP relaxations. *Proceedings of the 13th International Conference on Artificial Intelligence and Statistics*: 358-365.
- Li *et al.* (2008) Dynamic Bayesian network modeling of fMRI: a comparison of group-analysis methods. *Neuroimage* **41**(2):398-407.
- Loh, P.-L., Wainwright, M.J. (2013) Structure Estimation for Discrete Graphical Models: Generalized Covariance Matrices and Their Inverses. *Ann. Stat.* **41**(6):3022-3049.
- MacKay, D. (2003) *Information Theory, Inference and Learning Algorithms*. Cambridge University Press.
- Maathuis, M.H., Kalisch, M., Bühlmann, P. (2009) Estimating high-dimensional intervention effects from observational data. *Ann. Stat.* **37**(6A):3133-3164.
- Maher, B. (2012) ENCODE: The human encyclopaedia. *Nature* **489**(7414):46-48.
- Mechelli *et al.* (2002) Effective connectivity and intersubject variability: using a multisubject network to test differences and commonalities. *Neuroimage* **17**(3):1459-1469.
- Meinshausen, N., Bühlmann, P. (2006) High-dimensional graphs and variable selection with the lasso. *Ann. Stat.* **34**(3):1436-1462.
- Mohan *et al.* (2012) Structured sparse learning of multiple Gaussian graphical models. *Proceedings of the 26th Conference on Advances in Neural Information Processing Systems*: 620-628.
- Mukherjee, S., Speed, T. P. (2008) Network inference using informative priors. *Proc. Natl. Acad. Sci. USA* **105**(38):14313-14318.
- Mukherjee, S., Hill, S.M. (2011) Network clustering: probing biological heterogeneity by sparse graphical models. *Bioinformatics* **27**(7):994-1000.
- Nemhauser, G.L., Wolsey, L.A. (1988) *Integer and Combinatorial Optimization*. Wiley, New York.
- Niculescu-Mizil, A., Caruana, R. (2007) Inductive Transfer for Bayesian Network Structure Learning. *J. Mach. Learn. Res. Workshop and Conference Proceedings* **27**:339-346.
- Oates *et al.* (2013) Joint estimation of multiple networks from time course data. *CRiSM Working Paper, University of Warwick* **13**:3.
- Oates, C.J., Mukherjee, S. (2014) Joint Structure Learning of Multiple Non-Exchangeable Networks. *Proceedings of the 17th International Conference on Artificial Intelligence and Statistics*, to appear.
- Oates *et al.* (2014) Towards a Multi-Subject Analysis of Neural Connectivity. *CRiSM Working Paper, University of Warwick*.
- Oyen, D., Lane, T. (2013) Bayesian Discovery of Multiple Bayesian Networks via Transfer Learning. *arXiv*:1307.2312.
- Pearl, J. (2009) *Causality: models, reasoning and inference (2nd ed.)*. Cambridge University Press.

- Penfold *et al.* (2012) Nonparametric Bayesian inference for perturbed and orthologous gene regulatory networks. *Bioinformatics* **28**(12):i233-i241.
- Pensar *et al.* (2013) Labeled Directed Acyclic Graphs : a generalization of context-specific independence in directed graphical models. *arXiv*:1310.1187.
- Perrier, E., Imoto, S., Miyano, S. (2008) Finding Optimal Bayesian Network Given a Super-Structure. *J. Mach. Learn. Res.* **9**(10):2251-2286.
- Peters *et al.* (2011) Identifiability of Causal Graphs using Functional Models. *Proceedings of the 27th Conference on Uncertainty in Artificial Intelligence*: 589-598.
- Peters, J. Bühlmann, P. (2014) Structural Intervention Distance (SID) for Evaluating Causal Graphs. *arXiv*:1306.1043.
- Poldrack, R.A., Mumford, J.A., Nichols, T.E. (2011) *Handbook of fMRI Data Analysis*, Cambridge University Press.
- Queen, C.M., Albers, C.J. (2009) Intervention and causality: Forecasting traffic flows using a dynamic Bayesian network. *J. Am. Stat. Assoc.* **104**(486):669-681.
- Queen, C.M., Smith, J.Q. (1993) Multiregression dynamic models. *J. R. Statist. Soc. B* **55**(4):849-870.
- Ringach, D.L. (2009) Spontaneous and driven cortical activity: implications for computation. *Curr. Opin. Neurobiol.* **19**:439-444.
- Sachs *et al.* (2005) Causal protein-signaling networks derived from multiparameter single-cell data. *Science* **308**(5721):5239.
- Scheines, R., Hoihtink, H., Boomsma, A. (1999) Bayesian estimation and testing of structural equation models. *Psychometrika*, 64(1), 37-52.
- Scott, J.G., Berger, J.O. (2010) Bayes and Empirical-Bayes Multiplicity Adjustment in the Variable-Selection Problem. *Ann. Stat.* **38**(5):2587-2619.
- Sheehan *et al.* (2014) Maximum Likelihood Reconstruction of Very Large Pedigrees. *Theoretical Population Biology*, in submission.
- Silander, T., Myllymäkki, P. (2006) A simple approach to finding the globally optimal Bayesian network structure. *Proceedings of the 22nd Conference on Artificial Intelligence*: 445-452.
- Studený, M., Vomlel, J., Hemmecke, R. (2010) A geometric view on learning Bayesian network structures. *Int. J. Approx. Reason.* **51**(5):578-586.
- Studený, M., Haws, D. (2013) On Polyhedral Approximations of Polytopes for Learning Bayesian Networks. *J. Algebraic Stats.* **4**(1):59-92.
- Sugihara *et al.* (2006) Interindividual uniformity and variety of the “Writing center”: A functional MRI study. *Neuroimage* **32**(4):1837-1849.
- The Cancer Genome Atlas Network (2012) Comprehensive molecular portraits of human breast tumours. *Nature* **490**(7418):61-70.
- Thiesson *et al.* (1998) Learning mixtures of Bayesian networks. *Proceedings of the 14th Conference on Uncertainty in Artificial Intelligence*: 504-513.
- Tsamardinos, I., Brown, L.E., Aliferis, C.F. (2006) The max-min hill-climbing Bayesian network structure learning algorithm. *Mach. Learn.* **65**(1):31-78.

- Van Essen *et al.* (2013) The WU-Minn Human Connectome Project: An Overview. *Neuroimage* **80**:62-79.
- Werhli, A.V., Husmeier, D. (2008) Gene regulatory network reconstruction by Bayesian integration of prior knowledge and/or different experimental conditions. *Journal of Bioinformatics and Computational Biology* **6**(3):543-572.
- West, M., Harrison, P.J. (1997) *Bayesian Forecasting and Dynamic Models (2nd ed)*. Springer-Verlag, New York.
- Wolsey, L.A. (1998) *Integer Programming*. Wiley, New York.
- Xu *et al.* (2010) Inferring signaling pathway topologies from multiple perturbation measurements of specific biochemical species. *Sci. Sig.* **3**(113):ra20.
- Yang *et al.* (2012) Fused Multiple Graphical Lasso. *arXiv*:1209.2139.
- Yuan, C., Malone, B. (2013) Learning Optimal Bayesian Networks: A Shortest Path Perspective. *J. Artif. Intell. Res.* **48**:23-65.